

Frascati Physics Series Vol. nnn (2001), pp. 000-000

HEAVY QUARKS AT FIXED TARGET - Rio de Janeiro, Oct. 9-19, 2000

## THE LIGHT SCALARS, ESPECIALLY THE SIGMA, IN CHARM DECAY AND ELSEWHERE

N.A. Törnqvist and A. D. Polosa

*Physics Department, POB 9, FIN-00014, University of Helsinki, Finland*

### ABSTRACT

We discuss how the lightest scalars, in particular the broad  $\sigma$  resonance, can be understood as unitarized  $q\bar{q}$  states within a unitarized quark model (UQM). The bare  $q\bar{q}$  scalars are strongly distorted by hadronic mass shifts, and the  $u\bar{u} + d\bar{d}$  state becomes a very broad resonance, with its pole at 470-i250 MeV. This is the sigma meson required by models for spontaneous breaking of chiral symmetry. We also discuss the less well known phenomenon that with a large coupling there can appear two physical resonance poles on the second sheet although only one bare quark-antiquark state is put in. The  $f_0(980)$  and  $f_0(1370)$  resonance poles can thus be two manifestations of the same  $s\bar{s}$  quark state. Both of these are dominant in the E791 Dalitz plot of  $D_s \rightarrow 3\pi$ , where  $s\bar{s}$  intermediate states should be dominant. Recently this light  $\sigma$  has clearly been observed in  $D \rightarrow \sigma\pi \rightarrow 3\pi$  by the E791 experiment at Fermilab. We discuss how this decay channel can be predicted in a Constituent Quark Meson Model (CQM), which incorporates heavy quark and chiral symmetries.

## 1 Introduction

This talk is mainly based on earlier papers <sup>1, 2)</sup> on the light scalars and on a more recent one <sup>3)</sup> on the  $\sigma$  in charm decay, including a few new comments. First we shall discuss the evidence for the light  $\sigma$  and explain how one can understand the controversial light scalar mesons with unitarized quark model (UQM), which includes most well established theoretical constraints:

- Adler zeroes as required by chiral symmetry,
- all light two-pseudoscalar (PP) thresholds with flavor symmetric couplings in a coupled channel framework
- physically acceptable analyticity, and
- unitarity.

A unique feature of this model is that it simultaneously describes the whole scalar nonet and one obtains a good representation of a large set of relevant data. Only six parameters, which all have a clear physical interpretation, are needed, such as an overall coupling constant, the bare mass of the  $u\bar{u}$  or  $d\bar{d}$  state, the extra mass for a strange quark ( $m_s - m_u = 100$  MeV), a cutoff parameter ( $k_0 = 0.56$  GeV/c).

After describing our understanding of the  $q\bar{q}$  nonet, we discuss the recently measured  $D \rightarrow \sigma\pi \rightarrow 3\pi$  decay, where the  $\sigma$  is clearly seen as the dominant peak.

## 2 The problematic scalars and the existence of the $\sigma$

The interpretation of the nature of lightest scalar mesons has been controversial for long. There is no general agreement on where are the  $q\bar{q}$  states, is there a glueball among the light scalars, are some of the scalars multiquark or  $K\bar{K}$  bound states? As for the  $\sigma$ , authors do not even agree on its existence as a fundamental hadron, although the number of supporters is growing rapidly. A light scalar-isoscalar meson (the  $\sigma$ ), with a mass of twice the constituent  $u, d$  quark mass, or  $\approx 600$  MeV, coupling strongly to  $\pi\pi$  is of importance in all Nambu–Jona-Lasinio-like (NJL-like) models for dynamical breaking of chiral symmetry. In these models the  $\sigma$  field obtains a vacuum expectation value, i.e.,

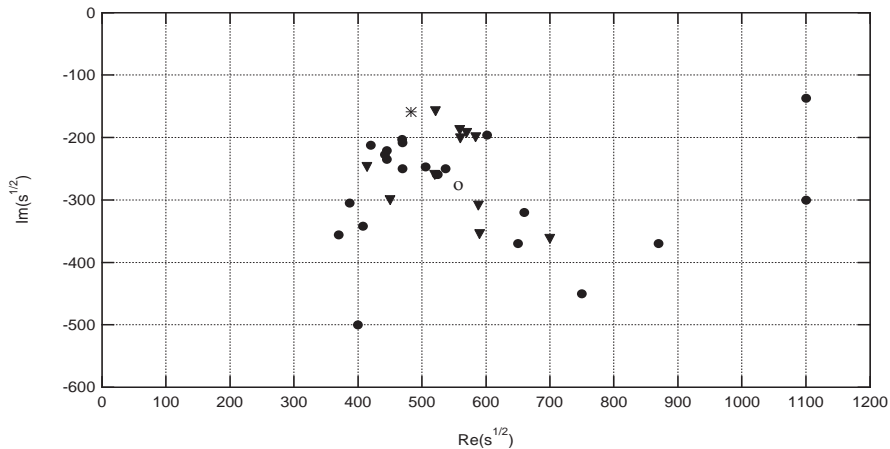


Figure 1: The pole positions of the  $\sigma$  resonance, as listed by the PDG <sup>4)</sup> under  $f_0(400-1200)$  or  $\sigma$  (filled circles), plotted in the complex energy plane (in units of MeV). The triangles represent the mass and width parameters (plotted as  $m - i\Gamma/2$ ), which were reported at this meeting. We could not here distinguish between pole and Breit-Wigner parameters. The star is the  $m - i\Gamma/2$  point obtained from the recent E791 experiment <sup>6)</sup> on  $D \rightarrow \sigma\pi \rightarrow 3\pi$  ( $m_\sigma = 478$  MeV,  $\Gamma_\sigma = 324$  MeV) while the open circle is that obtained by the CLEO analysis of  $\tau \rightarrow \sigma\pi\nu \rightarrow 3\pi\nu$  <sup>7)</sup>.

one has a  $\sigma q\bar{q}$  condensate in the vacuum, which is crucial for the understanding of all hadron masses, as it explains in a simple way the difference between the light constituent and chiral quark mass. Then most of the nucleon mass is generated by its coupling to the  $\sigma$ , which acts like an effective Higgs-like boson for the hadron spectrum.

In Fig. 1 we have plotted with filled circles the results of 22 different analyses on the  $\sigma$  pole position, which are included in the 2000 edition of the Review of Particle Physics <sup>4)</sup> under the entry  $f_0(400-1200)$  or  $\sigma$ . Most of these find a  $\sigma$  pole position near 500-i250 MeV.

Also, at a recent meeting in Kyoto <sup>5)</sup> devoted to the  $\sigma$ , many groups reported preliminary analyzes, which find the  $\sigma$  resonance parameters in the same region. These are plotted as triangles in Fig. 1. Here it was not possible to distinguish between Breit-Wigner parameters and pole positions, which of

course can differ by several 100 MeV for the same data. It must also be noted that many of the triangles in Fig. 1 rely on the same raw data and come from preliminary analyzes not yet published.

We also included in Fig. 1 (with a star) the  $\sigma$  parameters obtained from the recent E791 Experiment at Fermilab <sup>6)</sup>, where 46% of the  $D^+ \rightarrow 3\pi$  Dalitz plot is  $\sigma\pi$ . The open circle in the same figure represents the  $\sigma$  parameters extracted from the CLEO analysis of  $\tau \rightarrow \sigma\pi\nu \rightarrow 3\pi\nu$  <sup>7)</sup>.

### 3 The NJL and the linear sigma model

The NJL model is an effective theory which is believed to be related to QCD at low energies, when one has integrated out the gluon fields. It involves a linear realization of chiral symmetry. After bosonization of the NJL model one finds essentially the linear sigma model (L $\sigma$ M) as an approximate effective theory for the scalar and pseudoscalar meson sector.

About 30 years ago Schechter and Ueda <sup>8)</sup> wrote down the  $U3 \times U3$  L $\sigma$ M for the meson sector involving a scalar and a pseudoscalar nonet. This (renormalizable) theory has only 6 parameters, out of which 5 can be fixed by the pseudoscalar masses and decay constants ( $m_\pi$ ,  $m_K$ ,  $m_{\eta'}$ ,  $f_\pi$ ,  $f_K$ ). The sixth parameter for the OZI rule violating 4-point coupling must be small. One can then predict, with no free parameters, the tree level scalar masses <sup>9)</sup>, which turn out to be not far from the lightest experimental masses, although the two quantities are not exactly the same thing but can differ for the same model and data by over 100 MeV.

The important thing is that the scalar masses are predicted to be near the lightest experimentally seen scalar masses, and not in the 1500 MeV region where many authors want to put the lightest  $q\bar{q}$  scalars. The  $\sigma$  is predicted <sup>9)</sup> at 620 MeV with a very large width ( $\approx 600$  MeV), which well agrees with Fig. 1. The  $a_0(980)$  is predicted at 1128 MeV, the  $f_0(980)$  at 1190 MeV, and the  $K_0^*(1430)$  at 1120 MeV, which is surprisingly good considering that loop effects are large.

#### 4 Understanding the S-waves within a unitarized quark model (UQM)

In Figs. 2-4 we show the obtained fits to the  $K\pi$ ,  $\pi\pi$  S -waves and to the  $a_0(980)$  resonance peak in  $\pi\eta$ . The Partial Wave Amplitude (PWA) in the case of one  $q\bar{q}$  resonance, such as the  $a_0(980)$ , can be written as:

$$A(s) = -\frac{Im\Pi_{\pi\eta}(s)}{[m_0^2 + Re\Pi(s) - s + iIm\Pi(s)]}, \quad (1)$$

where:

$$\begin{aligned} Im\Pi(s) &= \sum_i Im\Pi_i(s) = -\sum_i \gamma_i^2 (s - s_{A,i}) \frac{k_i}{\sqrt{s}} e^{-k_i^2/k_0^2} \theta(s - s_{th,i}), \\ Re\Pi(s) &= \frac{1}{\pi} \text{P.V.} \int_{s_{th,1}}^{\infty} \frac{Im\Pi(s')}{s' - s} ds'. \end{aligned}$$

Here the coupling constants  $\gamma_i$  are related by flavour symmetry and OZI rule, such that there is only one over all parameter  $\gamma$ . The  $s_{A,i}$  are the positions of the Adler zeroes, which are near  $s = 0$ . Eq. (1) can be looked upon as a more general Breit-Wigner form, where the mass parameter is replaced by an  $s$ -dependent function, “the running mass”  $m_0^2 + Re\Pi(s)$ .

In the flavourless channels the situation is a little more complicated than in Eq. (1) since one has both  $u\bar{u} + d\bar{d}$  and  $s\bar{s}$  states, requiring a two dimensional mass matrix (see Ref. <sup>2)</sup>). Note that the sum runs over all light PP thresholds, which means three for the  $a_0(980)$ :  $\pi\eta$ ,  $K\bar{K}$ ,  $\pi\eta'$  and three for the  $K_0^*(1430)$ :  $K\pi$ ,  $K\eta$ ,  $K\eta'$ , while for the  $f_0$ 's there are five channels:  $\pi\pi$ ,  $K\bar{K}$ ,  $\eta\eta$ ,  $\eta\eta'$ ,  $\eta'\eta'$ .

In Fig. 5 we show, as an example, the running mass,  $m_0^2 + Re\Pi(s)$ , and the width-like function,  $-Im\Pi(s)$ , for the I=1 channel. The crossing point of the running mass with  $s$  gives the  $90^\circ$  mass of the  $a_0(980)$ . The magnitude of the  $K\bar{K}$  component in the  $a_0(980)$  is determined by  $-\frac{d}{ds} Re\Pi(s)$ , which is large in the resonance region just below the  $K\bar{K}$  threshold. These functions fix the PWA of Eq. (1) and Fig. 3. In Fig. 6 the running mass and width-like function for the strange channel are shown. These fix the shape of the  $K\pi$  phase shift and absorption parameters in Fig. 1. As can be seen from Figs. 1-3, the model gives a good description of the relevant data.

In Ref. <sup>2)</sup> the  $\sigma$  was missed because only poles nearest to the physical region were looked for, and the possibility of the resonance doubling phenomenon,

discussed below, was overlooked. Only a little later we realized with Roos<sup>1)</sup> that two resonances ( $f_0(980)$  and  $f_0(1370)$ ) can emerge although only one  $s\bar{s}$  bare state is put in. Then we had to look deeper into the second sheet and found the broad  $\sigma$  as the dominant singularity at low mass.

In fact, it was pointed out by Morgan and Pennington<sup>11)</sup> that for each  $q\bar{q}$  state there are, in general, apart from the nearest pole, also image poles, usually located far from the physical region. As explained in more detail in Ref.<sup>1)</sup>, some of these can (for a large enough coupling and sufficiently heavy threshold) come so close to the physical region that they make new resonances. And, in fact, there are more than four physical poles with different isospin, in the output spectrum of the UQM model, although only four bare states, of *the same nonet*<sup>1)</sup>, are put in!. The  $f_0(980)$  and the  $f_0(1300)$  of the model thus turn out to be two manifestations of the same  $s\bar{s}$  state. (See Ref.<sup>1)</sup> for details). There can be two crossings (see Fig. 7) with the running mass  $m_0^2 + \text{Re}\Pi(s)$ , one near the threshold and another at higher mass, and each one is related to a different pole at the second sheet (or, if the coupling is strong enough, the lower one could even become a bound state pole, below the threshold, on the first sheet).

Similarly the  $a_0(980)$  and the  $a_0(1450)$  could be two manifestations of the  $u\bar{d}$  state. Only after realizing that this resonance doubling is important the light and broad  $\sigma$  was found in the model<sup>1)</sup>. In Table 1 we list the pole positions of the six relevant poles, all manifestations of the same  $q\bar{q}$  nonet.

Another important effect that the model can explain is the large mass difference between the  $a_0$  and  $K_0^*$ . Because of this large mass splitting many authors argue that the  $a_0(980)$  and  $f_0(980)$  are not  $q\bar{q}$  states, since in addition to being very close to the  $K\bar{K}$  threshold, they are much lighter than the first strange scalar, the  $K_0^*(1430)$ . Naively one expects a mass difference between the strange and nonstrange meson to be of the order of the strange-nonstrange quark mass difference, or a little over 100 MeV.

Figs. 5 and 6 explain why one can easily understand this large  $K_0^*(1430) - a_0(980)$  mass splitting as a secondary effect of the large pseudoscalar mass splittings, and because of the large mass shifts coming from the loop diagrams involving the PP thresholds. If one puts Figs. 4 and 5 on top of each other one sees that the 3 thresholds  $\pi\eta$ ,  $K\bar{K}$ ,  $\pi\eta$  all lie relatively close to the  $a_0(980)$ , and all 3 contribute to a large mass shift. On the other hand, for the  $K_0^*(1430)$ ,

Table 1: The pole positions of the resonances in the S-wave  $PP \rightarrow PP$  amplitudes <sup>1)</sup>. The first resonance is the  $\sigma$  which we name here  $f_0(\approx 500)$ . The two following are both different manifestations of the same  $s\bar{s}$  state. The last entry is similarly an image pole of the  $a_0(980)$ , which in an improved fit could represent the  $a_0(1450)$ . The mixing angle  $\delta_S$  for the  $f_0(\approx 500)$  or  $\sigma$  is with respect to  $u\bar{u} + d\bar{d}$ , while for the two heavier  $f_0$ 's it is with respect to  $s\bar{s}$ .

| resonance          | $s_{\text{pole}}^{1/2}$ | $\delta_{S,pole}$     | Sheet  |
|--------------------|-------------------------|-----------------------|--------|
| $f_0(\approx 500)$ | $470 - i250$            | $(-3.4 + i1.5)^\circ$ | II     |
| $f_0(980)$         | $1006 - i17$            | $(0.4 + i39)^\circ$   | II     |
| $f_0(1370)$        | $1214 - i168$           | $(-36 + i2)^\circ$    | III,V  |
| $K_0^*(1430)$      | $1450 - i160$           | -                     | II,III |
| $a_0(980)$         | $1094 - i145$           | -                     | II     |
| $a_0(1450)?$       | $1592 - i284$           | -                     | III    |

the  $SU3_f$  related thresholds ( $K\pi$ ,  $K\eta'$ ) lie far apart from the  $K_0^*$ , while the  $K\eta$  nearly decouples because of the physical value of the pseudoscalar mixing angle.

This large mass of the  $K_0^*(1430)$  is also one of the reasons why some authors want to have a lighter strange meson, the  $\kappa$ , near 800 MeV. Cherry and Pennington <sup>10)</sup> recently have strongly argued against its existence. But, we heard Carla Göbel in her talk describing some evidence for such a light  $\kappa$  in the E791 data for  $D^+ \rightarrow K^- \pi^+ \pi^+$ . Here the signal is much less evident, since, differently from the case of the  $\sigma$ , which is seen as a clear peak over background, the inclusion of a  $\kappa$  only improves the  $\chi^2$  in the region dominated by the  $K^*(890)$ . Perhaps one should try a more sophisticated Breit-Wigner amplitude for the S-wave, as that in Eq. (1), before one can make more definite statements about the  $\kappa$ . Possibly such a light  $\kappa$  could be understood in connection to the resonance doubling phenomenon discussed above and which we discussed with Roos <sup>1)</sup>.

## 5 $D \rightarrow \sigma\pi \rightarrow 3\pi$

The recent experiments studying charm decay to light hadrons are opening up a new experimental window for understanding light meson spectroscopy and especially the controversial scalar mesons, which are copiously produced in these decays.

In particular we refer to the E791 study of the  $D \rightarrow 3\pi$  decay<sup>6)</sup> where it is shown how adding an intermediate scalar resonance with floating mass and width in the Monte Carlo program simulating the Dalitz plot densities, allows for an excellent fit to data provided the mass and the width of this scalar resonance are  $m_\sigma \simeq 478$  MeV and  $\Gamma_\sigma \simeq 324$  MeV. This resonance is a very good candidate for the  $\sigma$ . To check this hypothesis we adopt the E791 experimental values for its mass and width and using a Constituent Quark Meson Model (CQM) for heavy-light meson decays<sup>13)</sup> we compute the  $D \rightarrow \sigma\pi$  non-leptonic process via *factorization*<sup>14)</sup>, taking the coupling of the  $\sigma$  to the light quarks from the Linear sigma Model<sup>15)</sup>. In such a way one is directly assuming that the scalar state needed in the E791 analysis could be the quantum of the  $\sigma$  field of the Linear sigma Model. According to the CQM model and to factorization, the amplitude describing the  $D \rightarrow \sigma\pi$  decay can be written as a product of the semileptonic amplitude  $\langle \sigma | A_{(\bar{d}c)}^\mu(q) | D^+ \rangle$ , where  $A^\mu$  is the axial quark current, and  $\langle \pi | A_{\mu(\bar{u}d)}(q) | \text{VAC} \rangle$ . The former is parameterized by two form factors,  $F_1(q^2)$  and  $F_0(q^2)$ , connected by the condition  $F_1(0) = F_0(0)$ , while the latter is governed by the pion decay constant  $f_\pi$ . As far as the product of the two above mentioned amplitudes is concerned, only the form factor  $F_0(q^2)$  comes into the expression of the  $D \rightarrow \sigma\pi$  amplitude. Moreover we need to estimate it at  $q^2 \simeq m_\pi^2$ , that is the physically realized kinematical situation. The CQM offers the possibility to compute this form factor through two quark-meson 1-loop diagrams that we call the *direct* and the *polar* contributions to  $F_0(q^2)$ . These quark-meson loops are possible since in the CQM one has effective vertices (heavy quark)-(heavy meson)-(light quark) that allow us to *compute* spectator-like diagrams in which the external lines represent incoming or outgoing heavy mesons while the internal lines are the constituent light quark and heavy quark propagators.

In Figs. 8 and 9 we show respectively the *direct* and the *polar* diagrams for the semileptonic amplitude  $D \rightarrow \sigma$ , the former being characterized by the axial current directly attached to the constituent quark loop, the latter involving an



intermediate  $D(1^+)$  or  $D(0^-)$  state. These two diagrams are computed with an analogous technique and one finally obtains a determination of the direct and polar form factors  $F_0^{\text{dir,pol}}(q^2)$ . The extrapolation to  $q^2 \simeq m_\pi^2 \simeq 0$  is safe for the direct form factor while is not perfectly under control for the polar form factor since the latter is more reliable at the pole  $q^2 \simeq m_P^2$ ,  $m_P$  being the mass of the intermediate state in Fig. 9. We take into account the uncertainty introduced by this extrapolation procedure and signaled by the fact that we find  $F_0^{\text{pol}}(0) \neq F_1^{\text{pol}}(0)$  (computing  $F_0$  from the polar diagram with  $0^-$  intermediate polar state and  $F_1$  from that with intermediate  $1^+$  state). Our estimate for  $F_0(0) = F_0^{\text{pol}}(0) + F_0^{\text{dir}}(0) = 0.59 \pm 0.09$  is in reasonable agreement with an estimate of  $F_0(m_\pi^2) = 0.79 \pm 0.15$  carried out in <sup>16)</sup> using the E791 data analysis and a Breit-Wigner like approximation for the  $\sigma$ .

The meson-quark loops in Figs. 8 and 9 are computed substituting the meson vertices with the heavy meson field expressions found by Heavy Quark Effective Theory (HQET) (since CQM incorporates heavy quark and chiral symmetries) and the quark lines with the propagators of the heavy and light constituent quarks. The light constituent mass  $m$  is fixed by a NJL-type gap equation that depends on  $m$ , and on two cutoffs  $\Lambda$  and  $\mu$  in a proper time regularization scheme for the diverging integrals. The ultraviolet cutoff  $\Lambda$  is fixed by the scale of chiral symmetry breaking,  $\Lambda_\chi \simeq 4\pi f_\pi$ , and we consider  $\Lambda = 1.25$  GeV. The remaining dependence of  $m$  on the choice of the infrared cutoff  $\mu$  has an expression similar to that of a ferromagnetic order parameter,  $m(\mu)$  being different from zero for  $\mu$  values smaller than a particular  $\mu_c$ , and zero for higher values. When  $\mu$  ranges from 0 to 300 MeV, the value of  $m$  is almost constant,  $m = 300$  MeV, dropping for higher  $\mu$  values. A reasonable light constituent quark mass is certainly 300 MeV and this clearly leaves a 300 MeV open window for choosing the infrared cutoff. Enforcing the kinematical condition for the meson to decay to its free constituent quarks, which must be possible since the CQM model does not incorporate confinement, requires  $\mu \simeq m$  <sup>13)</sup>. Therefore we pick up the  $\mu = 300$  MeV value. The results are quite stable against 10 – 15% variations of the UV and IR cutoffs.

The CQM semileptonic  $D \rightarrow \sigma$  transition amplitude is represented by the loop integrals associated to the direct and to the polar contributions. The result of the integral computations must then be compared with the expression for the hadronic transition element  $\langle \sigma | A | D \rangle$  and this allows to extract the desired

$F_{0,1}$  form factors. An estimate of the weight of  $1/m_c$  corrections can also be taken into account <sup>3)</sup>.

This computation indicates that the scalar resonance described in the E791 paper can be consistently understood as the  $\sigma$  of the Linear sigma Model. Of course a calculation such as the one here described calls for alternative calculations and/or explanations of the E791 data for a valuable and useful comparison of point of views on the  $\sigma$  nature.

## 6 Concluding remarks

An often raised question is: Why are the mass shifts required by unitarity so much more important for the scalars than, say, for the vector mesons? The answer is very simple, and there are three main reasons:

- The scalar coupling to two pseudoscalars is very much larger than the corresponding coupling for the vectors, both experimentally and theoretically (e.g., spin counting gives 3 for the ratio of the two squared couplings).
- For the scalars the thresholds are S-waves, giving nonlinear square root cusps in the  $\Pi(s)$  function, whereas for the vectors the thresholds are P-waves, giving a smooth  $k^3$  angular momentum and phase space factor.
- Chiral symmetry constraints, in particular Adler zeroes, are important for the scalars when analyzing pseudoscalar scattering, and make, e.g.,  $\pi\pi \rightarrow \pi\pi$  very weak near the thresholds. In the case when a light scalar is produced in charm decay, as in E791, these zeroes are less important.

One could argue that the two states  $f_0(980)$  and  $a_0(980)$  are a kind of  $K\bar{K}$  bound states (see Ref. <sup>12)</sup>), since these have a large component of  $K\bar{K}$  in their wave functions. However, the dynamics of these states is quite different from that of normal two-hadron bound states. If one wants to consider them as  $K\bar{K}$  bound states, it is the  $K\bar{K} \rightarrow s\bar{s} \rightarrow K\bar{K}$  interaction which creates their binding energy, not the hyperfine interaction as in Ref. <sup>12)</sup>. Thus, although they may spend most of their time as  $K\bar{K}$ , they owe their existence to the  $s\bar{s}$  state. Therefore, it is more natural to consider the  $f_0(980)$  and  $f_0(1300)$  as two manifestations of the same  $s\bar{s}$  state.

The wave function of the  $a_0(980)$  (and  $f_0(980)$ ) can be pictured as a relatively small core of  $q\bar{q}$  of typical  $q\bar{q}$  meson size (0.6 fm), which is surrounded by a much larger standing S-wave of virtual  $K\bar{K}$  (see Fig. 10) due to the fact that these resonances are just below the  $K\bar{K}$  threshold and they strongly couple to  $K\bar{K}$ . This picture also gives a physical explanation of the narrow width: in order to decay to  $\pi\eta$ , the  $K\bar{K}$  component must first virtually annihilate near the origin to  $q\bar{q}$ . Then the  $q\bar{q}$  can decay to  $\pi\eta$  as an OZI allowed decay.

Finally, in Sec. 5, we showed that the recent E791 data on  $D \rightarrow \sigma\pi$  can be understood in the CQM model assuming the  $\sigma$  to be predominantly a  $(u\bar{u} + d\bar{d})/\sqrt{2}$  state, similar to the  $\sigma$  of the Linear sigma Model.

## 7 Acknowledgements

NAT and ADP acknowledge support from EU-TMR programme, contract CT98-0169. The authors are also grateful to A. Deandrea, R. Gatto and G. Nardulli for useful discussions.

## References

1. N.A. Törnqvist and M. Roos, Phys. Rev. Lett. **76**, 1575 (1996).
2. N.A. Törnqvist, Z. Phys **C68**, 647 (1995); N. A. Törnqvist, Eur. J. Phys. **C11**, 359 (1999).
3. R. Gatto, G. Nardulli, A.D. Polosa and N.A. Törnqvist, hep-ph/0007207, in press in Phys. Lett. **B**.
4. D.E. Groom et al. Eur. J. Phys. **C 15**, 1 (2000).
5. Conference: "Possible existence of the light  $\sigma$  resonance and its implications to hadron physics", Kyoto, Japan 11-14th June 2000, KEK-proceedings/2000-4; See also N.A. Törnqvist, "Summary of the conference", hep-ph/0008135.
6. E. M. Aitala et al. (E791 collaboration), *Experimental evidence for a light and broad scalar resonance in  $D^+ \rightarrow 3\pi$* , hep-ex/0007028.
7. D.M. Asner *et al.* (CLEO collaboration), Phys. Rev. **D61**, 0120002 (1999).
8. J. Schechter and Y. Ueda, Phys. Rev. **D3**, 2874 (1971).

9. N.A. Törnqvist, Eur. J. Phys. **C11**, 559 (1999); M. Napsuscia, hep-ph/9803396; see also G. Parisi and M. Testa Nuov. Cim. **LXVII**, 13 (1969).
10. S. N. Cherry and M. Pennington, hep-ph/0005208.
11. D. Morgan and D. Pennington, Phys. Rev. **D48**, 1185 (1993); *ibid.* **D48**, 5422 (1993).
12. J. Weinstein and N. Isgur, Phys. Rev. Lett. **48**, 659 (1982); Phys. Rev. Lett. **27**, 588 (1983).
13. A.D. Polosa, *The CQM model*, hep-ph/0004183 and references therein.
14. M. Bauer, B. Stech and M. Wirbel, Z. Phys. **C16**, 205 (1983).
15. D. Ebert and M.K. Volkov, Z. Phys. **C16**, 205 (1983).
16. C. Dib and R. Rosenfeld, *Estimating  $\sigma$  meson couplings from  $D \rightarrow 3\pi$  decays*, hep-ph/0006145.

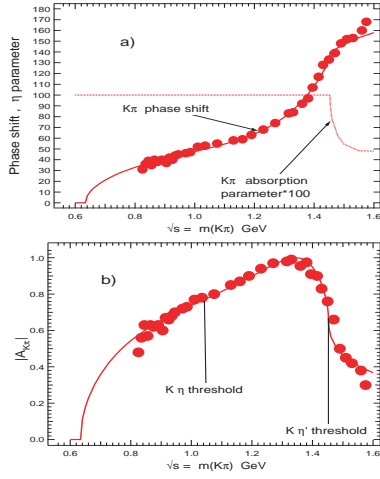


Figure 2: The  $K\pi$   $S$ -wave phase shift and (b) the magnitude of the  $K\pi$  PWA compared with the model predictions, which fix 4 ( $\gamma$ ,  $m_0+m_s$ ,  $k_0$  and  $s_{A,K\pi}$ ) of the 6 parameters.

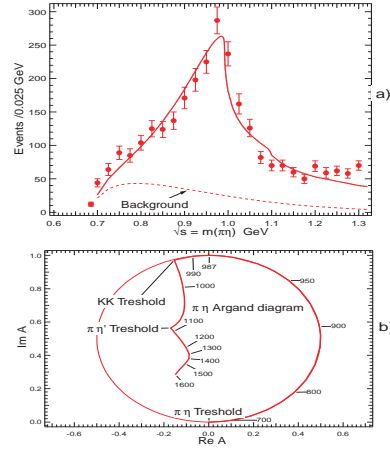


Figure 4: (a) The  $a_0(980)$  peak compared with model prediction and (b) the predicted  $\pi\eta$  Argand diagram.

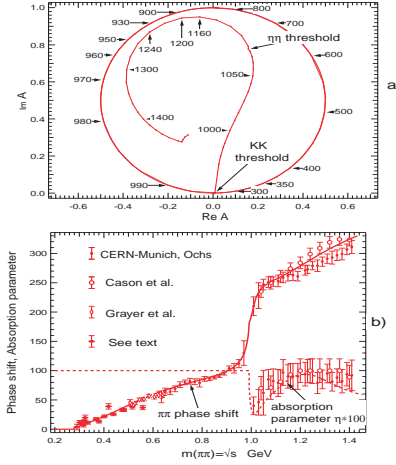


Figure 3: (a) The  $\pi\pi$  Argand diagram and (b) phase shift predictions are compared with data. Note that most of the parameters were fixed by the data in Fig. 1. For more details see Ref. <sup>1,2</sup>.

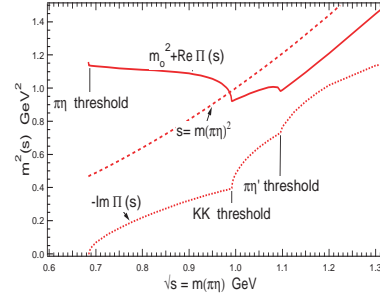


Figure 5: The running mass  $m_0 + \text{Re}\Pi(s)$  and  $\text{Im}\Pi(s)$  of the  $a_0(980)$ . The strongly dropping running mass at the  $a_0(980)$  position, below the  $K\bar{K}$  threshold contributes to the narrow shape of the peak in Fig. 3a.

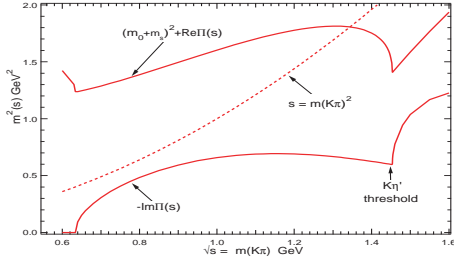


Figure 6: The running mass and width-like function  $-\text{Im}\Pi(s)$  for the  $K_0^*(1430)$ . The crossing of  $s$  with the running mass gives the  $90^\circ$  phase shift mass, which roughly corresponds to a naive Breit-Wigner mass, where the running mass is put constant.

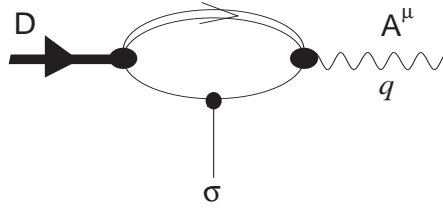


Figure 8: Diagram for the direct contribution to the  $D \rightarrow \sigma$  semileptonic amplitude. The axial current is directly attached to the quark loop.

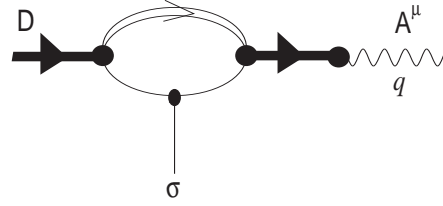


Figure 9: The polar contribution to  $F_0$ , if a  $0^-$  intermediate state is considered, and to  $F_1$ , with a  $1^+$  intermediate state. The  $D(1^+)$  state is described in the PDG <sup>4</sup>.

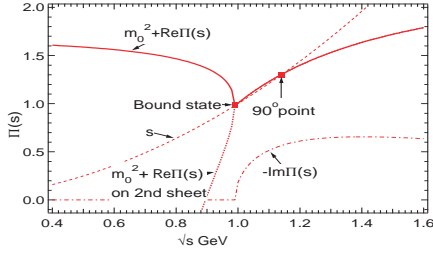


Figure 7: (a) Although the model has only one bare  $s\bar{s}$  resonance, when unitarized it can give rise to two crossings with the running mass in the  $s\bar{s} - K\bar{K}$  channels. This means the  $s\bar{s}$  state can manifest itself in two physical resonances, one at threshold and one near 1200 MeV (See Ref. <sup>2</sup> for details) as in this figure.

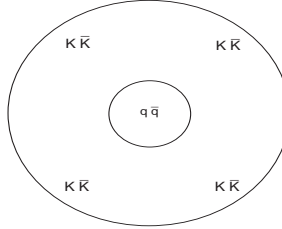


Figure 10: A resonance just below the  $K\bar{K}$  threshold, coupling strongly to  $K\bar{K}$ , must have a large  $K\bar{K}$  standing wave surrounding a  $q\bar{q}$  core.